

Dear Author,

Please, note that changes made to the HTML content will be added to the article before publication, but are not reflected in this PDF.

Note also that this file should not be used for submitting corrections.



Contents lists available at ScienceDirect

Composite Structures

journal homepage: www.elsevier.com/locate/compstruct



Low velocity impact and CAI of woven carbon fibre reinforced highly polymerized thermoplastic epoxy modified with submicron diameter glass fibres

Valter Carvelli ^{a,*}, Hironori Nishida ^b, Toru Fujii ^c, Kazuya Okubo ^c

^a Department of A.B.C., Politecnico di Milano, Milan, Italy

^b Hiroshima Prefectural Technology Research Institute, Kure, Hiroshima, Japan

^c Department of Mechanical Engineering, Doshisha University, Tatara Kyotanabe, Kyoto, Japan

ARTICLE INFO

Article history:

Received 17 September 2019

Revised 2 December 2019

Accepted 30 December 2019

Available online xxxxx

Keywords:

Thermoplastic epoxy

Carbon fibre

Submicron diameter glass fibres

Impact

CAI

Damage tolerance

ABSTRACT

The experimental study aimed to understand the effect of the highly polymerized thermoplastic epoxy matrix and of the submicron diameter glass fibres content on the impact and compression after impact (CAI) performance of woven carbon fibre reinforced composites. A thermoset epoxy system was also considered for the sake of comparison. The comparison highlighted the better impact performance of the composites with the thermoplastic epoxy matrix of higher weight-average molecular weight (Mw), which is further improved by the proper content of micro glass fibres. The enhanced impact damage tolerance was also demonstrated observing the damage imparted with surface laser morphology, infrared thermography and X-ray μ -CT.

© 2019 Published by Elsevier Ltd.

1. Introduction

Long and continuous fibre reinforced composite materials have been used in several industrial applications, having excellent potential for reducing weight, as well as lifetime maintenance costs owing to their corrosion and mechanical properties [1].

However, composites are costly and difficult to repair when exposed to impact damage. Composite structures are more vulnerable to impact damage than similar metallic ones. They are sensitive to low velocity impact, which could produce diffuse internal damages, while leaving negligible damage on the impact surface [2]. Among the sequence of impact damage modes [3], intra-ply damage (resin cracking and fiber/matrix interfacial debonding) and inter-ply damage (interlaminar delamination) are dominant damage modes under a low-energy impact. Fibre breakage is the dominant failure mode under high-energy impact. The internal damage after impact could develop under loadings and could cause severe strength reductions and catastrophic failure. Hence, understanding impact mechanical behaviour, energy absorbing capabilities and impact resistance of composites are the major concerns for

improving the impact damage tolerance and to prevent ultimate failure of composite structures [1].

Factors affecting the impact resistance and damage tolerance of composite materials can be divided into primary and secondary [2,3]. The primary factors, having the most significant effect, are the characteristics of the resin system and fibre, the fibre/matrix interface and the reinforcement architecture. The resin system is the topic of this paper. Secondary factors include: environmental-related conditions, stacking sequence, fibre hybridization, repeated impact, etc. [2].

As for the primary factors, on one hand, many studies were conducted to improve the impact resistance with different fibre materials [4] and changing the reinforcement architecture, e.g. stitching or 3D fabrics to improve the through the thickness reinforcement (see [5–7]). On the other hand, the attention was focused on developing resin systems with improved mechanical properties [8–10]. For more than four decades, thermoset resin (TS) systems were extensively used for manufacturing composite components due to their ease manufacturing and improved mechanical/thermal properties. However, their weaknesses such as brittleness, long processing cycle, non-recyclability (irreversible exothermic chemical reaction during curing) draw the attention of the composite industry to use thermoplastic resin (TP) systems [10]. Under impact loading, thermoplastic matrix systems could provide

* Corresponding author.

E-mail address: valter.carvelli@polimi.it (V. Carvelli).

enhanced toughness owing to higher damage onset energy and ultimate energy than that of thermoset systems [3].

The main advantage of thermoplastic resins (TP) compared to thermoset (TS) counterpart are: increased toughness, better recyclability due to the physical change in the shape upon heating, and mainly the ability to deliver fast manufacturing processes. However, available TP resins have higher melt viscosity than TS ones. Hence, the infusion process with conventional TP resins could lead to inappropriate impregnation of the yarns.

Recently, a thermoplastic epoxy resin (TP epoxy) was developed with both advantages of thermoset and thermoplastic resins [11]. It has the good workability of thermoset resins and the formability and recyclability of thermoplastic systems. In previous studies, this thermoplastic epoxy was adopted for manufacturing textile carbon fibre reinforced thermoplastic epoxy composites (CFRTP), and to study the effect of the weight-average molecular weight (Mw) on quasi-static and fatigue mechanical performance [12]. The studies highlighted the better properties of high Mw TP composites with improved tensile strength and longer tensile-tensile fatigue life. Moreover, the CFRTP had an enhanced fracture toughness (mode I and mode II) compared to the TS counterpart, namely a thermoset epoxy resin reinforced with the same carbon textile (CFRTS). The improved damage resistance of the composite driven by the properties of the TP epoxy matrix could suggest a better impact performance and a better retention of the mechanical properties after impact.

Over the past decades, being impact behaviour of composite materials highly influenced by the matrix, research efforts were dedicated to improve the toughness of resin systems, mainly thermoset ones (see e.g. [13,14]). Modified thermosetting matrices for fibre reinforced composites have evolved greatly over the past three decades in overcoming the brittle nature of thermosetting polymers by dispersion of a second phase that normally consists of nano- or micro- sized fillers (such as nanotubes, fibres, particles, rubber, etc) (see e.g. [15–19]). Fillers are expected to provide extrinsic toughening mechanisms [20] and, as consequence, to positively affect the mechanical response of fibre reinforced composites [21]. In particular, employing submicron diameter fibres improved the fracture characteristics of matrices and composites, acting as a reinforcing phase at the nano/micro-scale [22].

The present study aims to assess the impact tolerance of the highly polymerized thermoplastic epoxy carbon textile composite compared to the TS counterpart. Moreover, the effects of hybrid epoxy systems, modified with submicron diameter glass fibres, on the impact performance was studied.

Drop weight impact tests were performed on composites with the two resin systems, assuming an impact energy of 30 J. The impact damage extension was observed by laser microscope morphology and thermal measurements, as well as, X-ray micro-Computed Tomography (μ -CT). The residual mechanical strength after impact was measured by compression after impact test (CAI).

2. Composites components and manufacturing

2.1. Matrices, reinforcement and micro fibres

Thermoplastic epoxy resin (DENATITE XNR 6850A) and the accelerator (XNH 6850B) were supplied by Nagase ChemteX Corporation, Japan [11]. The intrinsic properties of thermoplastic epoxy resin and accelerator are listed in Table 1 (according to the producer [11]) and T_g is approximately 100 °C.

For the sake of comparison, thermoset epoxy resin (JER828, Mitsubishi Chemical Corporation) and amine (JER113, Mitsubishi Chemical Corporation) were used as resin and curing agent, respectively.

Table 1
Properties of thermoplastic epoxy resin and accelerator.

	DENATITE XNR6850A	accelerator XNH6850B
Chemical classification	Formulated epoxy resin	Aromatic phosphoric acid ester
Aspect	White paste	White powder
Viscosity at 25 °C	220 Pa s	Solid
Specific Gravity at 25 °C	1.17	1.10

Plain weave carbon fibre fabric (Mitsubishi Rayon TR3110MS) was used as reinforcement (yarn TR30S 3L, linear density 1.79 g/cm³, pick and end counts 12.5 per inch, areal weight 200 g/m², according to the producer). The textile reinforcement was selected for the high fibres and matrix adhesion surface, leading to a considerable influence of the matrix on the mechanical behaviour of the composites.

Submicron diameter glass fibres had cross-section radius of 0.25 μ m and average length of 150 μ m, supplied by Nippon Muki Corporation, Japan.

2.2. Manufacturing of prepreg

Plain weave CFRTP prepreg preparation had the following steps. The resin, 'XNR 6850A', was heated by using an electric oven at 120 °C. When the temperature of the resin reached 105 °C, the accelerator 'XNH 6850B' was added to the resin with stirring. Then micro glass fibres of the considered weight content (0.1% and 0.3% in weight of resin) was mixed in the thermoplastic epoxy system by a homogenizer, 5000 rpm for 10 min. The plain weave carbon fabric was impregnated with the thermoplastic epoxy resin by hand lay-up. The Mw of prepreg was finally controlled by a predetermined time and temperature sequence [23], namely for some ranges of Mw (k means thousand): 15k < Mw < 40k, 30 min at 100 °C; 45k < Mw < 65k, 30 min at 150 °C; Mw > 70k, >60 min at 150 °C.

2.3. Manufacturing of laminates

CFRTP prepreps, obtained by impregnation with the thermoplastic epoxy resin in the state of oligomer, were dried at 50 °C for 12 h, and then stacked to create CFRTP laminates with 14 layers. The curing was in a hot-press moulding at 175 °C and 6 MPa. The CFRTP laminates had fibre volume fraction and thickness of approximately 40% and 4.01 \pm 0.25 mm (average and standard deviation of 42 measurements), respectively.

The same plain weave carbon fibre fabric was used as reinforcement of the thermoset resin. The CFRTS plates with 14 layers were laminated by hand lay-up impregnation. The mould was cured in a hot press at 80 °C for 1 h and then at 150 °C for 3 h. The CFRTS laminates had approximately 40% fibre volume fraction and thickness of 4.02 \pm 0.19 mm (average and standard deviation of 15 measurements).

Preliminary studies [12,24] highlighted the effect of the weight-average molecular weight (Mw) on mechanical properties of the same carbon textile composite, showing the better properties for Mw higher than 50k–60k (k means thousand). Therefore, in the present study, two or three molecular weights (lower, close to and higher than the transition level) of the thermoplastic epoxy system were selected to assess the effect on the impact performance compared to the thermoset counterpart. The micro glass fibres contents (percentage of the resin weight) and the weight-average molecular weights (Mw) of the thermoplastic epoxy matrix are listed in the synopsis of the adopted composite materials in Table 2.

Table 2
Micro glass fibres content and weight-average molecular weight (Mw) of thermoplastic epoxy composite materials ('k' means thousand).

Micro glass fibres content [%]	Weight-average molecular weight (Mw)		
0	41k	68k	
0.1	32k	48k	88k
0.3	29k	48k	74k

The identification of each material, in the following, contains three sets for the thermoplastic epoxy composites, namely: TP-(Mw)-(glass fibres content %). While for the thermoset epoxy composites, the ID has two sets: TS-(glass fibres content %). IDs without the glass fibres content indicate unmodified matrices.

3. Experimental program and features

The experimental campaign concerned some preliminary tests and the impact related activities. Preliminary measurements were limited to mode II interlaminar fracture toughness, being an important damage mode during impact, and IZOD impact test for initial understanding on the effect of Mw and of micro glass fibres modification of matrix. The limited quantity of the materials did not allow to perform all considered measurements for all combinations of matrices, Mw and glass fibres contents. This did not affect the meaning and understandings of the study.

3.1. Preliminary measurements

3.1.1. Weight-average molecular weight

The weight-average molecular weight of the thermoplastic epoxy matrix was measured for each batch by the gel permeation chromatography (GPC) adopting a CLASS-LC10 (Shimadzu Corporation) and a GPC column (Styragel HR4E, Styragel HR5E: waters). Tetrahydrofuran (THF) was used as solvent. The calibration curves were drawn based on the retention time and the Mw of standard polystyrene.

3.1.2. End notched flexure (ENF), mode II inter-lamina fracture toughness

The laminate, prepared for ENF test, had 20 layers of plain weave carbon fabric. Five specimens for each considered Mw (length 140 mm, width 25 mm, thickness 5.5 mm) were subjected to quasi-static three-point bending loading, according to the standard [25]. Four and two Mws were adopted for the unmodified and 0.3% micro glass fibre modified thermoplastic epoxy composite, respectively. The length of pre-crack was 50 mm. Kapton film of approximately 30 μm thick (Kapton, Du Pont-Toray Corporation) was inserted between 10th and 11th ply of the laminate. The Mode II inter-lamina fracture toughness was determined at 0.5 mm/min of cross-head speed, and calculated according to [25].

3.1.3. Izod impact strength

Izod impact tests were conducted using an impact pendulum (Yonekura seisaku-sho, Co., Ltd., A1040). Specimens were prepared with 14 layers of plain weave carbon fabric and had length 80 mm and width 10 mm. Unmodified matrix and 0.1%, 0.3% micro glass fibres modified thermoplastic epoxy were considered, with the Mw listed in Table 2 (for 0.1%, only the two higher Mws). The Izod impact test was according to the standard [26]. The impact was for ten unnotched specimens of each material.

3.2. Impact tests

Drop weight impact test was according to [27], with a hemispherical striker tip of 20 mm diameter. The adopted impact device

was CEAST FractoVis 6789. For the sake of comparison, an impact energy of 30 J was selected, setting the impactor mass of 6.153 kg and impactor drop height of 0.497 m. The specimen (100 × 60 mm²) was clamped by a system with an inner hole diameter of 40 mm, and impacted at the centre. The recorded impactor velocity at the initial contact was 3.122 m/s (low-velocity impact event [3]). The rebound catcher system was enabled to stop the impactor during its second descent. At least three specimens for each material were used for impact test.

3.3. Compression tests

Compression strength, before and after impact, was measured according to [28], by a Shimadzu universal material testing machine (load cell 50 kN), cross head speed of 1 mm/min.

Three specimens for each material, Mw, and micro glass fibres content were used for compression after impact, while two specimens for compression strength before impact due to the reduced quantity of available materials.

3.4. Devices for damage assessment

To assess the damage imparted during impact, the morphology of the impacted surface was detected by a shape measurement laser microscope KEYENCE VK-X210. Measurements were adopted to get the dent depth.

Moreover, an infrared thermo camera TESTO 890 (accuracy 0.01 °C) was used to monitor the evolution of the temperature on the specimen impacted surface opposite to the heating source. The distance between the camera's lens and the specimen surface was approximately 1 m. The heating source was applied for 5 s using an infrared lamp (electric power of 2.5 kW) positioned at about 20 cm from the specimen. Images of the impacted surface (resolution 640 × 480 pixels) were continuously recorded for 12 s, with a frequency of 20 Hz, from the beginning of the heating. They provided the heterogeneous diffusion (conduction) of the thermal front into the material as results of the impact damage. The specimen was set in a 4 cm thick frame of expanded polystyrene during heating and temperature recording, to limit as much as possible the boundary effects.

The internal damage after impact was also visualized by X-ray μ-CT using a SkyScan 1172 system, with images of 1000 × 1000 pixels and pixel size of 26.8 μm.

4. Results of the preliminary tests

Preliminary measurements were dedicated to the mode II inter-lamina fracture toughness and Izod impact to get a first insight on the effect of Mw and of modification of the thermoplastic matrix by micro glass fibres. The tests selection was motivated being mode II delamination one of the main damage mode during impact, and to get the range of impact strength by easy to perform unmonitored Izod impact.

4.1. Mode II inter-lamina fracture toughness

The effect at the layers interface of the Mw and 0.3% micro glass fibre content was estimated measuring the mode II inter-lamina fracture toughness of the laminate. The unmodified thermoplastic epoxy composite showed, as reported in [12], almost linear increase of the mode II inter-lamina fracture toughness with the Mw (Fig. 1), which is consequence of the better adhesion of the carbon fibre and highly polymerized thermoplastic epoxy matrix [12]. The unmodified thermoset reinforced composite had fracture toughness comparable to the thermoplastic one of 60k Mw, almost half than the value for the higher considered Mw of 108k.

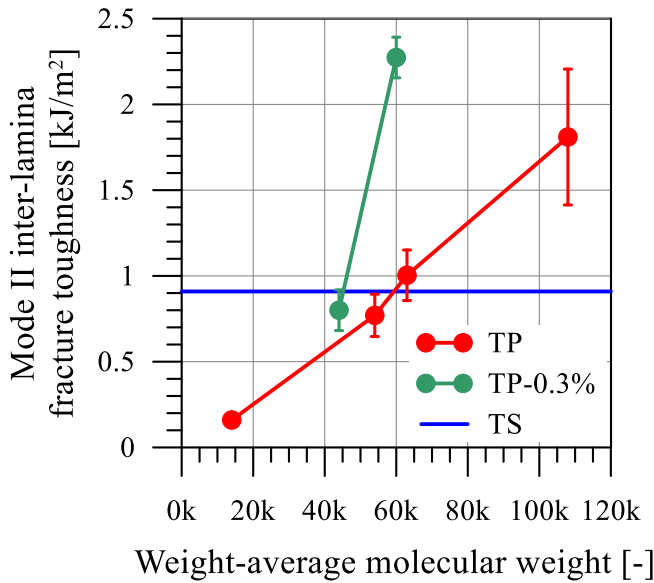


Fig. 1. Mode II inter-lamina fracture toughness of unmodified (TP) and modified 0.3% micro glass fibres (TP-0.3%) thermoplastic composite, and unmodified thermoset epoxy composite (TS). 'k' means thousand and error bars indicate standard deviation.

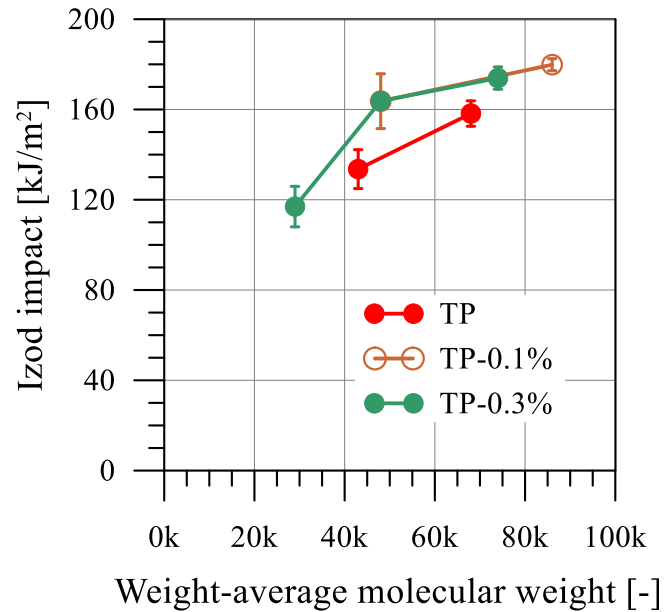


Fig. 2. Izod impact strength of unmodified (TP) and modified 0.1%, 0.3% micro glass fibres (TP-0.1%, TP-0.3%) thermoplastic composite. 'k' means thousand and error bars indicate standard deviation.

The modification of the thermoplastic resin with the micro glass fibres generated an improvement of the fracture toughness (Fig. 1) with a considerable increase for Mw in the transition range of about 60k [12]. This could be motivated by the presence of the micro glass fibres, which develops toughening mechanisms such as crack bridging and/or crack-pinning [20].

4.2. Izod impact strength

The enhancement of the Izod impact strength increasing the Mw of the thermoplastic epoxy is shown in Fig. 2, both for unmodified and modified resin system. For the sake of comparison, as reported in [24], the impact strength of the unmodified thermoset resin composite had an average value of 108 kJ/m². The micro glass fibre in the thermoplastic epoxy got an increment of the impact strength in the range 10–20%. Increasing the micro glass fibre content from 0.1% to 0.3% did not get a variation of the impact strength (Fig. 2).

Side view of the failure modes of the impacted specimens are shown in Fig. 3. Diffuse through the thickness delamination and long cracks in the specimen length direction are visible for the lower Mw of the unmodified thermoplastic composite (TP-41k). Increasing the Mw and the content of micro glass fibres, the failure was characterized by few and short delamination (Fig. 3, higher Mw). The reduced delamination of TP higher Mw composite (TP-68k), comparing to lower Mw (TP-41k) and TS counterpart, was clearly visible by SEM observations (Fig. 4). It is clearly connected to the enhancement of the mode II inter-lamina fracture toughness highlighted in Fig. 1. As mentioned in [12], the deformation of the TP resin system with high Mw improved the 'ductility' of the matrix allowing for a better redistribution of the stress field ahead of the crack tip and an improvement of the fracture toughness. The latter is enhanced with the micro glass fibres, which offered bridging action, delaying crack propagation.

5. Results and comparison of impact

Impact tests were conducted assuming an impact energy of 30 J. It did not lead to perforation, for all considered materials, but

allowed initiation and development of different damage modes and the measurement of the residual compression strength. The effect of the thermoplastic epoxy Mw and micro glass fibres content, as well as the epoxy resin system (thermoplastic and thermoset), on the impact performance was assessed considering different measurements during the impact test (e.g. force, energy and deflection, namely displacement of the spherical impactor). The damage imparted was compared by the morphology of the impacted surface and by the heterogeneous distribution of the heating propagation. To quantitatively compare the extension of the damage surface, a preliminary estimation method is detailed assuming the temperature recordings. Moreover, internal damage was visualized by X-ray μ -CT.

5.1. Impact performance

The force and energy evolution during impact of unmodified thermoplastic and thermoset epoxy reinforced composites shows considerable differences (see Fig. 5a). The TP composites of both Mw had different shapes of the force versus time curve since the first discontinuity of the slope (F_1). The TS and the TP of lower Mw (41k) had almost similar damage initiation (matrix crack) force level (F_1), with drop of the force for the former, probably due to larger number of cracks, and a variation of slope with increasing force for the latter, meaning a more gradual initiation and development of the damage in the matrix. Comparing TS to the unmodified TP of higher Mw (68k), the latter had variation of slope (initiation of matrix crack) for considerably higher load level.

The shift in time of the maximum energy of the TS compared to TP composites (Fig. 5a) could represent a different evolution and a wider extension of the damage.

The post peak of TS had several drops of the force, indicating more severe damage events occurred (several unstable delaminations), while TP-41k had a gradual descending branch with smaller drops of the force, with probably less extended cracks and delamination. On the contrary, the TP-68k had a post peak gradually and continuously descending, which could reflect a more 'ductile' and damage tolerant behaviour of the TP high Mw matrix (Fig. 5a).

The recording of the force vs. deflection (Fig. 5b) revealed a similar maximum deflection of the two TP composites, which was

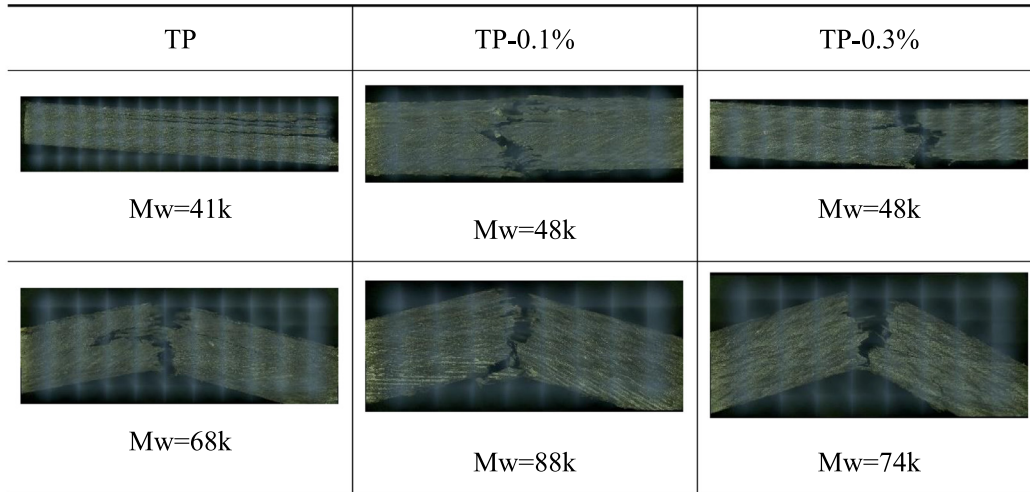


Fig. 3. Izod impact strength: side view of failure mode.

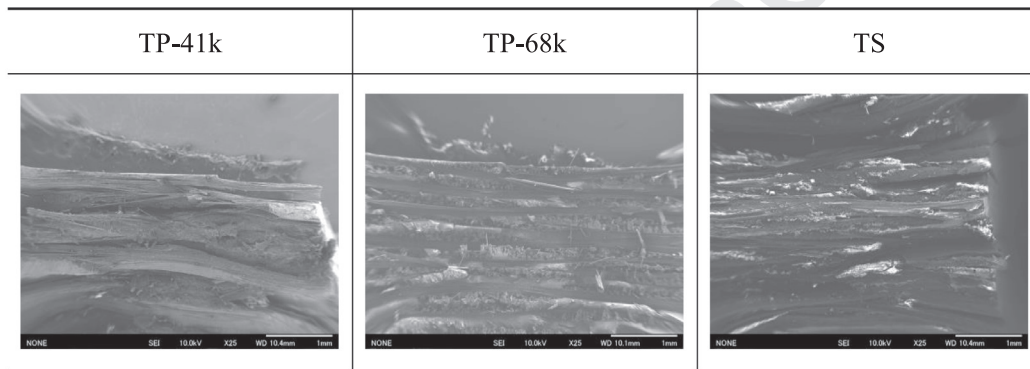


Fig. 4. Izod impact strength: SEM observation of the fracture surface.

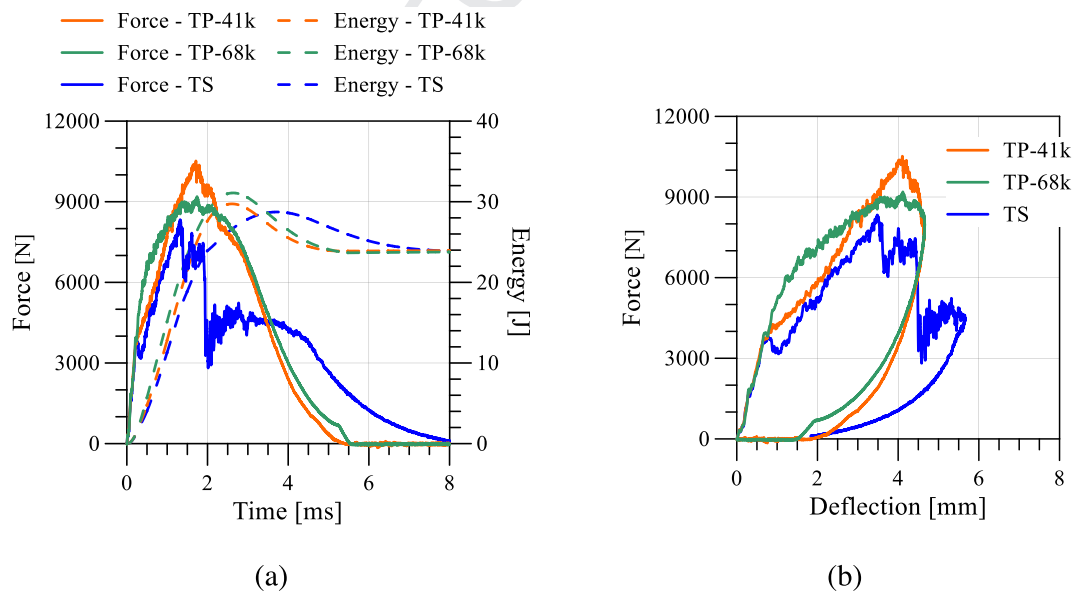


Fig. 5. Impact: representative comparison of unmodified TP and TS composites: (a) force and energy vs. time; (b) force vs. deflection.

377 smaller than the one experienced in the TS. It had a higher deflection
378 as consequence of the more diffuse damage in the material.

379 The modification of the TP epoxy with 0.1% content of micro
380 glass fibres did not have a considerable effect on the impact

response (Fig. 6). The lower Mw (32k) had quite similar response
to the TS, in term of matrix damage initiation and post peak drops
of the force. The main variations are due to the increase of the Mw
(48k and 88k), which changed the damage initiation force level, the

381
382
383
384

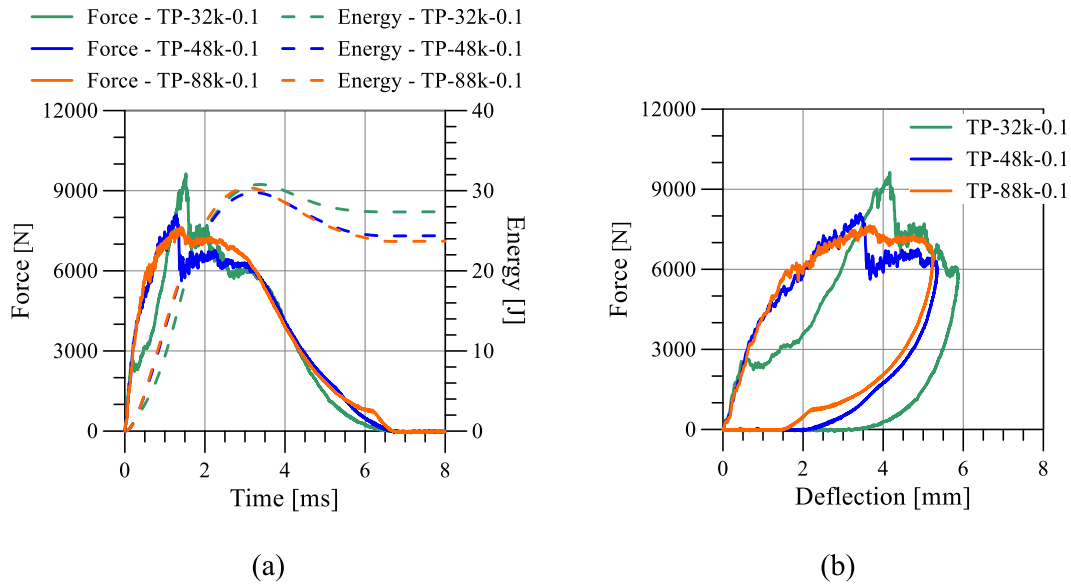


Fig. 6. Impact: representative comparison of 0.1% micro glass fibres modified TP composites: (a) force and energy vs. time; (b) force vs. deflection.

maximum force, and the descending branch with increasing 'ductile' behaviour for the Mw of 88k. Similar observations are for the maximum deflection, which decrease increasing the Mw. It predicts a less impact damage tolerance for low Mw TP composites modified with the 0.1% micro glass fibres.

Increasing the content of micro glass fibres up to 0.3% (Fig. 7) lead to almost similar impact response for medium and high Mw. The micro fibres had a positive effect on the lower Mw composite (29k), getting similar, to the higher Mw, damage initiation force and damage evolution phase, post peak branch of force vs. time, while it had slightly higher absorbed energy resulting in different damage level (see X-ray μ -CT).

The effect of micro glass fibres content on low and high Mw is summarized in Figs. 8 and 9, respectively. As for low Mw (Fig. 8), the matrix modification slightly increased the matrix damage initiation. The 0.1% content worsened the post peak with abrupt reductions of load, comparing to the unmodified material (TP-

32k-0.1, Fig. 8a), and higher maximum deflection (Fig. 8b). The 0.3% content compensated the lower fracture toughness of the low TP Mw composite, leading to a similar impact behaviour compared to the unmodified material, both in term of post peak and deflection (Fig. 8), although the latter had a higher absorbed energy and probably a more extended damage pattern.

The 0.1% content of micro glass fibres in the higher Mw TP composite (TP-88k-0.1, Fig. 9) deteriorated the impact behaviour with a lower maximum force, a higher deflection and irregular drops of the load in the post peak, indications of less 'ductility' and less damage tolerance compared to the unmodified material. The 0.3% content slightly modify the macroscopic impact behaviour of the TP composite (TP-74k-0.3, Fig. 9), having similar evolution of force, energy and deflection.

An overview of the effect of matrix (TP and TS) with the same 0.3% content of micro glass fibres is detailed in Fig. 10. It is clear the enhanced impact performance of the TP reinforced carbon

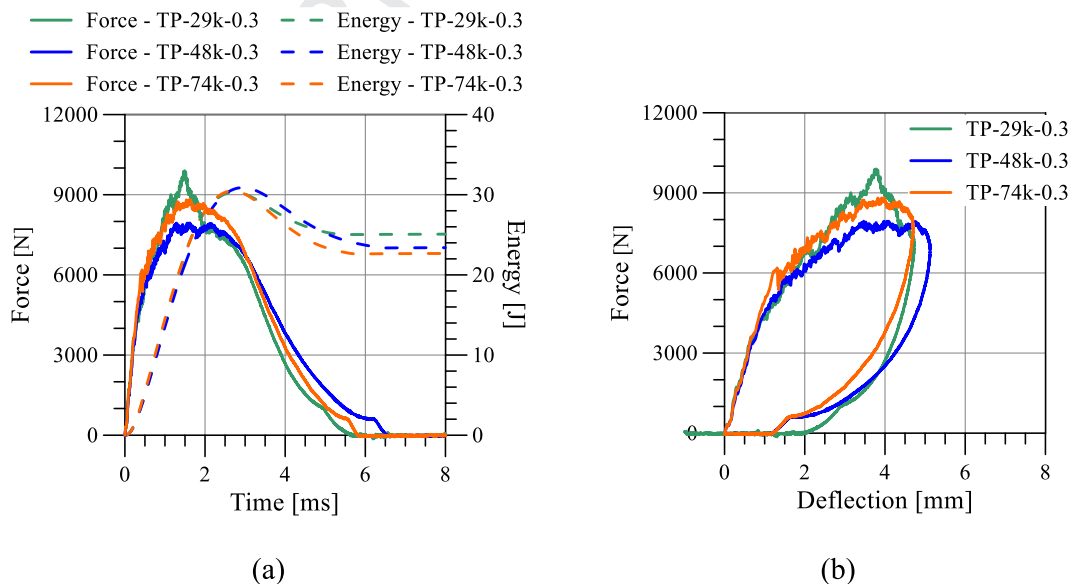


Fig. 7. Impact: representative comparison of 0.3% micro glass fibres modified TP composites: (a) force and energy vs. time; (b) force vs. deflection.

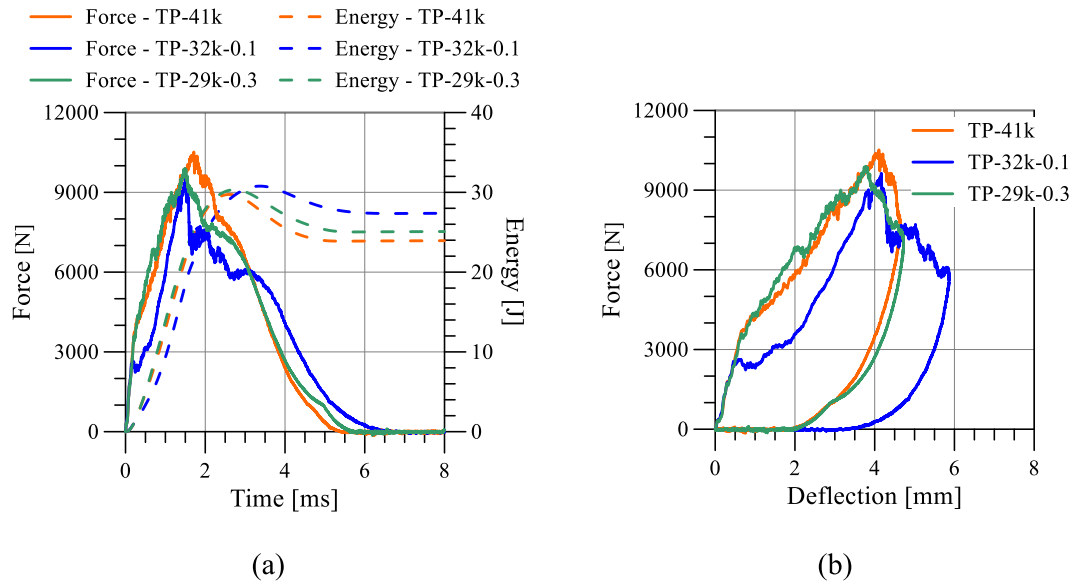


Fig. 8. Impact: representative comparison of lower Mw unmodified, and 0.1%, 0.3% micro glass fibres modified TP composites: (a) force and energy vs. time; (b) force vs. deflection.

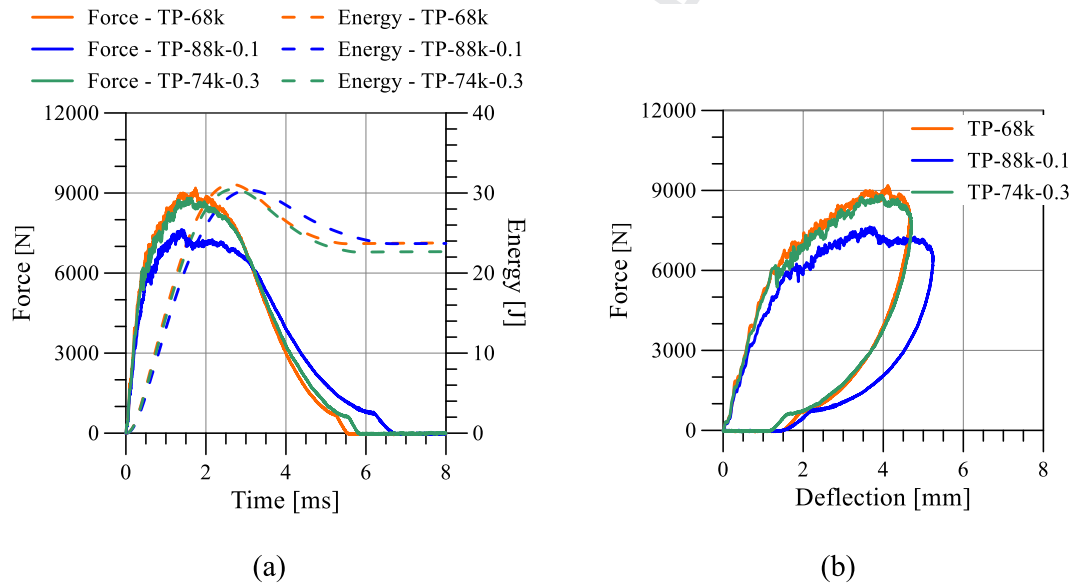


Fig. 9. Impact: representative comparison of higher Mw unmodified, and 0.1%, 0.3% micro glass fibres modified TP composites: (a) force and energy vs. time; (b) force vs. deflection.

419 composite for both Mw. TP composites had higher load for matrix
420 damage initiation, smooth and more 'ductile' post peak, mainly for
421 the higher Mw (TP-74k-0.3), with lower absorbed energy and
422 smaller maximum deflection (Fig. 10b).

423 Considering the complete set of recorded diagrams, an overview
424 and comparison of the impact performance of the considered com-
425 posites is detailed assuming the main parameters (Fig. 11),
426 namely: force at first slope variation (damage initiation) (F_1) and
427 maximum peak force (F_{max}); elastic energy ($E_{elastic}$) and absorbed
428 energy ($E_{absorbed}$); maximum deflection. The load level F_1 had
429 almost same value for both unmodified TS and TP composites ir-
430 respective of the Mw, meaning similar damage initiation load level.
431 The micro glass fibres modification did not change the latter level
432 for the TS composite, while F_1 increased increasing the Mw for the
433 modified TP composites. As observed above, the 0.1% content did

not improve the low Mw matrix properties, showing the lower
434 level for damage initiation (TP-32k-0.1, Fig. 11a). A higher Mw
435 and/or 0.3% of micro glass fibres allowed an enhanced tolerance
436 of the damage initiation, with load levels higher than the unrein-
437 forced materials counterpart. As for the maximum force of the TS
438 composites, it was not modified by the micro glass fibres. Differ-
439 ently, the F_{max} of the TP composites decreased with increasing
440 the Mw for both unmodified and micro glass fibres modified ma-
441 terials. It had a reduction of 11% from 48k to 68k for the unmodified
442 TP, of 24% from 32k to 88k for 0.1% modified TP, and of 7% from 29k
443 to 74k for 0.3% modified TP. This reduction had generally as conse-
444 quence a modification of the post peak behaviour with more 'duc-
445 tile' behaviour of the higher Mw TP composites (see e.g. Figs. 5-7).
446

The micro glass fibres modification of the TS matrix created a
447 slight increase of the absorbed energy of the composites, meaning
448

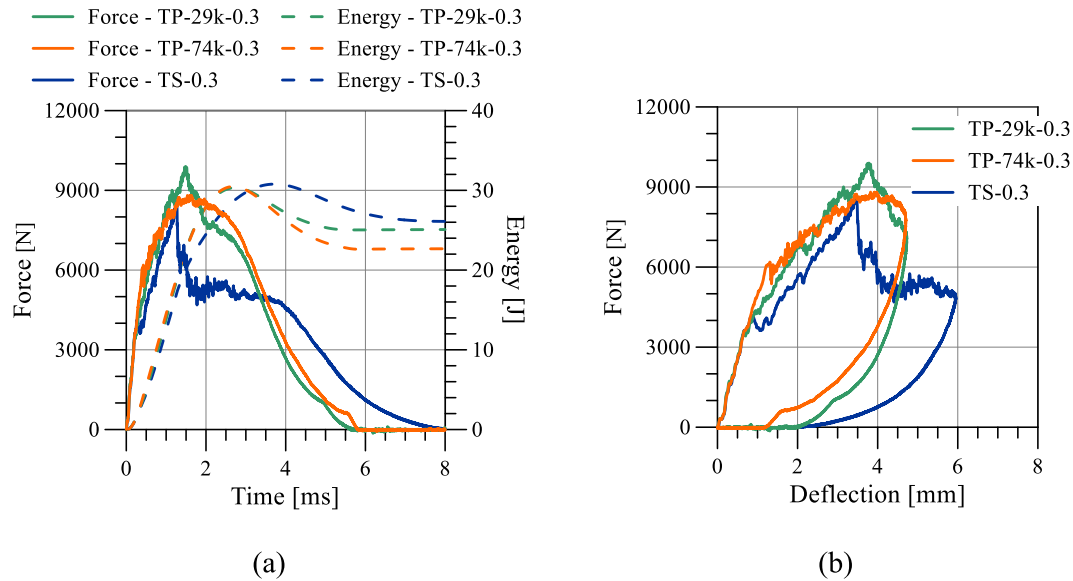


Fig. 10. Impact: representative comparison of 0.3% micro glass fibres modified TP and TS composites: (a) force and energy vs. time; (b) force vs. deflection.

more energy dedicated to the damage development (Fig. 11b). Except the 0.1% content of micro glass fibres, the TP composites had level of absorbed energy lower than the TS counterparts. Moreover, a reduced absorbed energy was for the higher Mw. The latter had higher level of elastic energy as consequence of the relative lower energy dedicated to the damage propagation (Fig. 11b). It still highlighted the better impact damage tolerance of the high Mw TP composites, unmodified and 0.3% modified matrices.

The maximum deflection (Fig. 11c) under the low velocity impact provided similar information, as it is connected to the absorbed energy, and as consequence to the imparted damage. The deflection is generally lower for the unmodified and 0.3% modified TP composites than the TS materials (Fig. 11c). It was expected having lower level of absorbed energy. It was not for the 0.1% modified TP composites, for which, as stated above, the content of micro glass fibres did not help to improve the fracture toughness of the TP matrix, mainly for low Mw.

5.2. After impact laser surface morphology

The laser measurement of the impacted surface provided an initial insight of the imparted damage. The density and distribution of the cracks showed a larger damage area with wider cracks for the TS composites both for unmodified and modified resin (see Fig. 12d,e). The TP composites had different morphology according to the Mw and micro fibres contents. Fig. 12 details only the higher Mw materials having the better impact performance. On one hand, the higher Mw TP composite with 0.1% content of micro glass fibres had wider and longer cracks (TP-88k-0.1, Fig. 12b) as TS counterpart. It is connected to the higher level of absorbed energy and deflection (Fig. 11). On the other hand, the unmodified and 0.3% modified higher Mw TP composites had relatively lower density of damage (Fig. 12a and c). Moreover, the 0.3% modified TP composite showed also the shortest cracks length (see TP-74k-0.3, Fig. 12c), which highlights the better impact tolerance, as reflected by the residual maximum deflection (dent depth, Fig. 13). The dent depth could be a predictive mark of the residual mechanical features of the composite. All 0.1% modified composites had the highest dent depth, as expected from the morphology in Fig. 12b. The resin modification did not reduce the residual

deformation of the TS composite (increased of 20%), while a reduction was recorded for the TP counterpart increasing the Mw (reduction of 13% from 48k to 74k Mw). The main advantage of the 0.3% modification of the TP resin was observed for the Mw ≥ 48k. The latter had 34% smaller dent depth than the lower Mw (29k), and generally the lowest of the considered composites (Fig. 13), which still confirm the better damage tolerance with reduced residual deformation of the TP composite modified with 0.3% of micro glass fibres.

5.3. After impact thermography

Infrared thermography was adopted to assess the correlation of the damage imparted and the temperature evolution of the impacted surface. To eliminate the influence of environment interference and sensitivity of apparatus on thermal measurements ([29]), the temperature distribution at time 0.1 sec from the beginning of heating (supposed for 5 sec) was subtracted to that of each image at any recording time. It gives the variation of temperature (ΔT) with respect to the beginning of heating. The here detailed and compared variation of temperature maps of the impacted surface are supposed after 10 sec since the beginning of the heating, namely 5 sec after the heating ending.

Although the specimen was set in a 4 cm thick frame of expanded polystyrene, the heating diffusion at the boundary created an inhomogeneous distribution with a reduction of ΔT at the boundary of about 0.5 °C compared to the centre part of the specimen, as visible for a material before impact in Fig. 14a.

The heat flux had a heterogeneous propagation due to the difference of thermal conductivity between the undamaged and damage material (Fig. 14b). The discontinuities created by the imparted cracks in the damaged area slow the heat flux, while it is faster in the undamaged material. As consequence, the damaged area showed a lower temperature compared to the undamaged portion (Fig. 14b).

Thermographs of all TS composites clearly distinguish the damage and undamaged portion of the specimens, showing the expected damaged circular area as imparted by the spherical impactor (Fig. 15c and d). Similar was recorded for the low Mw TP composites (see e.g. Fig. 14b for TP-32k-0.1). The different damage mode of the high Mw TP composites resulted in a completely

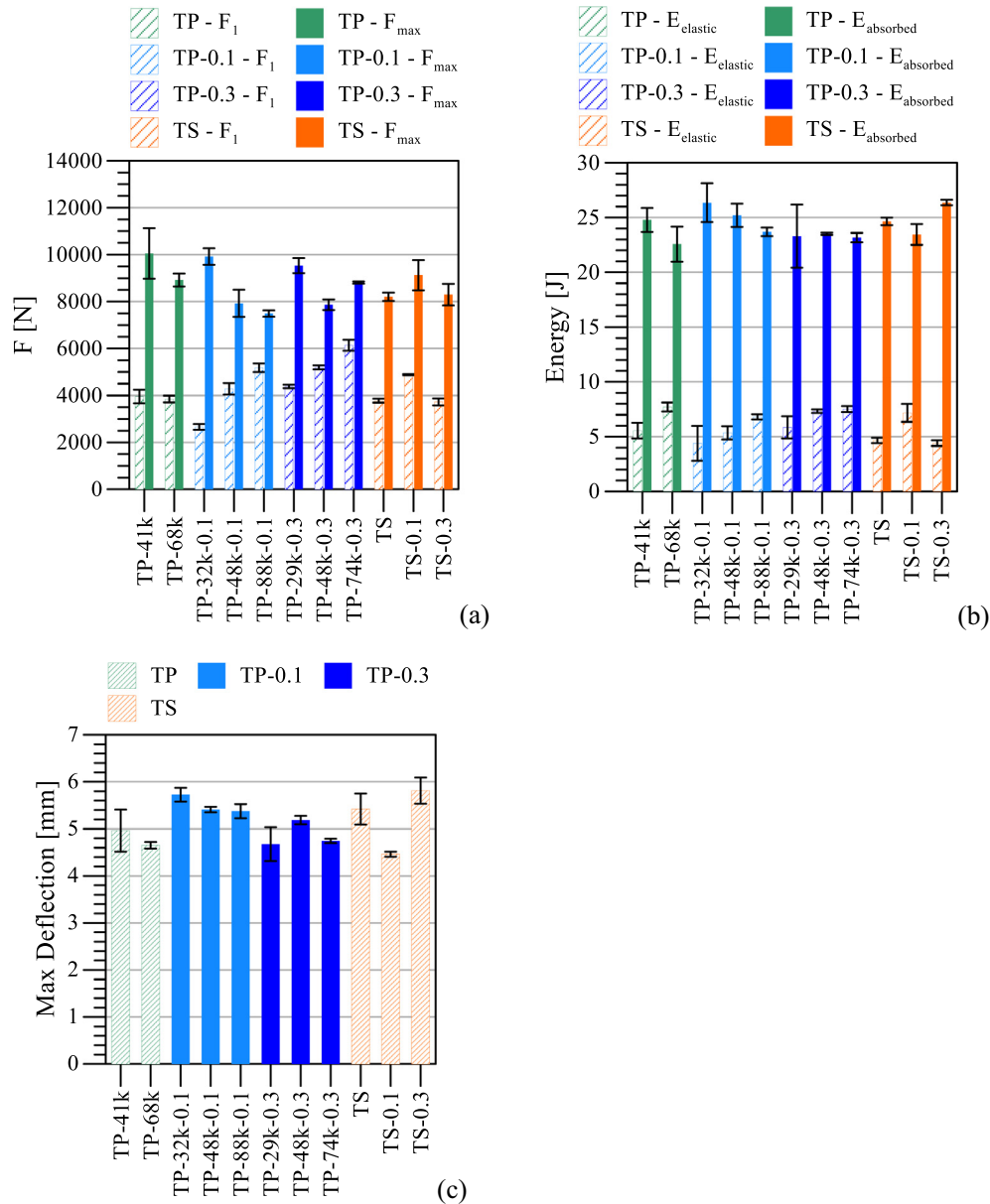


Fig. 11. Impact: comparison of: (a) force at first change of force-displacement initial slope (F_1), and maximum force (F_{max}); (b) elastic and absorbed energy; (c) maximum deflection. Average and standard deviation (error bars) of three tests.

527 different temperature distribution, as compared to TS and low Mw
 528 TP composites. The lower density and size of cracks (see Fig. 12a
 529 and c, X-Ray μ -CT) in the materials with high Mw TP did not gener-
 530 ate a considerable variation of the through the thickness thermal
 531 conductivity of the damage portion, leading to an almost uniform
 532 distribution of the ΔT on the impacted surface (Fig. 15a and b),
 533 considering the mentioned boundary effect. The ‘plastic’ deforma-
 534 tion of the high Mw TP epoxy, observed in [12], reduced thought
 535 the thickness and in-plane cracks propagation. This effect was
 536 enhanced with the 0.3% content of micro glass fibres with a further
 537 crack bridging effect. Therefore, the different damage mode of the
 538 high Mw TP composites (see X-ray μ -CT), mainly thought the
 539 thickness, did not allow a distinction of the damage and undam-
 540 aged material by the thermograph recording. It confirms the better
 541 damage tolerance of the high Mw TP composites, compared to the
 542 TS counterpart, resulting in a reduction of the cracks propagation,

543 which did not lead to a considerable variation of the through the
 544 thickness macro thermal conductivity.

5.4. Preliminary size estimation of damaged area

545
 546 The thermography of impacted specimens was adopted to have
 547 a preliminary quantitative estimation of the extension of the damage
 548 surface after impact. The estimation is based on the distribu-
 549 tion of the temperature $\Delta T(x,y)$ (see e.g. Fig. 16a) connected to
 550 the damage and undamaged material, as consequence of the sup-
 551 posed variation of the thermal conductivity of the damage zone.
 552 The technique to distinguish the latter was adapted from the one
 553 detailed in [30]. It is based on the definition of a threshold temper-
 554 ature ΔT_S leading to a good binary representation of the heated
 555 area (580×350 pixels, picture portion outside the specimen was
 556 removed). All pixel temperatures below this threshold belong to

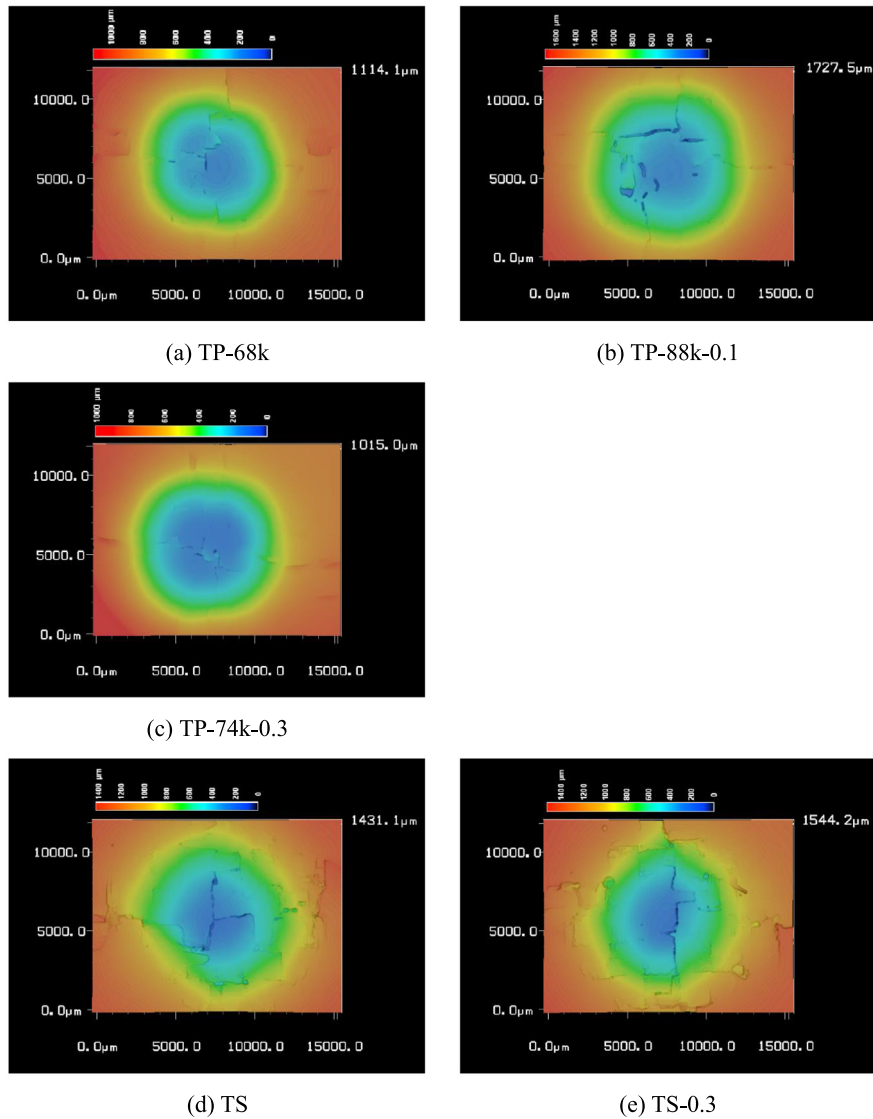


Fig. 12. After impact laser profilometer. Impacted surface profile: higher Mw (a) TP unmodified, (b) TP 0.1% and (c) TP 0.3% modified composites; (d) TS unmodified and (e) TS 0.3% modified composites.

the damaged area, whereas all values above the threshold belong to the undamaged area of the specimen. This leads to the binarization by the definition of the matrix of the damage $\underline{M}_D(x, y)$, as:

$$\underline{M}_D(x, y) = \begin{cases} 1 & \text{if } \Delta T(x, y) \leq \Delta T_S \text{ damaged} \\ 0 & \text{if } \Delta T(x, y) > \Delta T_S \text{ undamaged} \end{cases} \quad (1)$$

The estimation of the threshold temperature starts with the histogram of actual temperature values of the considered thermogram (Fig. 16b). The temperatures of the pixels were distributed into classes of 0.1 °C, over the whole temperature range of the thermogram. The histogram displays the temperature with maximum frequency $\Delta T_{max-freq}$ and its frequency h_{max} . The width at half of this peak ($h_{max}/2$) is considered to determine the left temperature border as the threshold temperature (adapted from [30]):

$$\Delta T_S = \Delta T \left(\frac{h_{max}}{2} \right)_{left} \quad (2)$$

Finally, the visualization of the matrix of the damage (Eq. (1)) clearly distinguish the damaged area (Fig. 16c), which well corresponds to the temperature variation of the impacted area.

The size of the damaged area A_D could be easily calculated by counting the number of pixels with a value of 1:

$$A_D = \sum_{x,y} \underline{M}_D(x, y) \quad (3)$$

Boundary effects could lead to lower temperature close to the specimen border (see top right of Fig. 16c). This could be erroneously considered as damage by the above procedure. To exclude those undamaged regions, the calculation of damage area is restricted to a subdomain (see yellow rectangle in Fig. 16c).

The above procedure is not suitable when the imparted damage does not create a variation of the through the thickness thermal conductivity, resulting in an almost uniform distribution of the temperature over the specimen surface, as was recorded for the

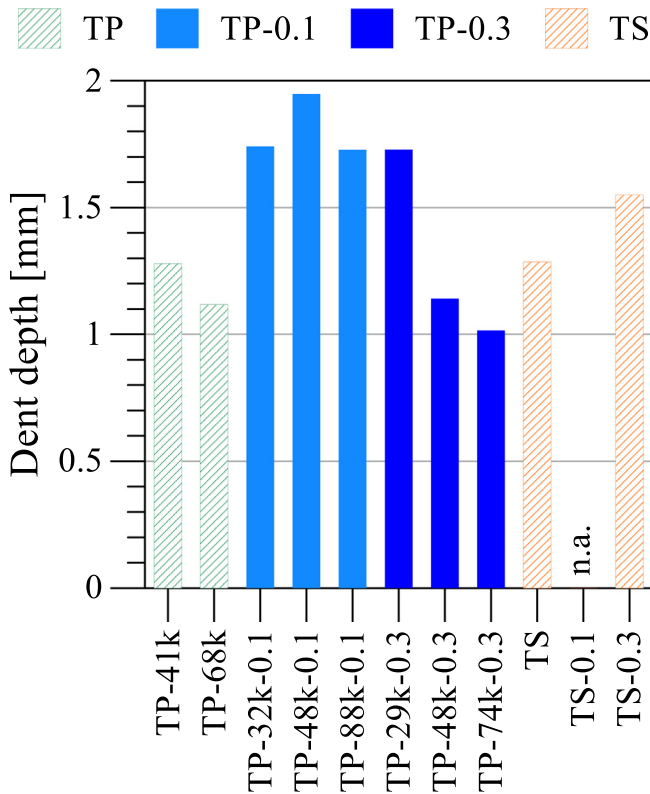


Fig. 13. After impact laser profilometer: dent depth. Average of two measurements.

higher Mw of the TP composites (see e.g. Fig. 15a and b). It leads to a narrow distribution in the histogram of the pixels' temperatures and a small number of them below the threshold temperature, which generally are in an undamaged region close to the specimen border, see e.g. estimation in Fig. 17 for the specimen TP-74k-0.3 of Fig. 15b.

This procedure provided the estimation of the damaged area detailed in Fig. 18, only for the thermograms of the impacted specimens with a heterogeneous distribution of the surface temperature, due to the damage pattern. The ratio of damage area A_D/A_{Tot} (being A_{Tot} the total surface of the specimen) did not have considerable variation for the TS composites, although the micro glass fibres modifications. It was in the range 10–12%. The unmodified low Mw (41k) TP composites had a similar extension of the damaged area, approximately 13%, which considerably decreased, of about 38%, for similar Mw (48k) and 0.1 content of micro glass fibres. While, TP with the lower Mw (29k) and 0.3% of glass fibres had a ratio of damaged area of about 6.5% with a reduction with respect to the unmodified counterpart TP composite of about 50%. This still highlights the contribution of the micro glass fibres in improving the impact damage tolerance of low Mw TP composites, with compensation of their low fracture toughness (Fig. 1).

However, it must be underlined that it is a preliminary procedure which needs improvements and mainly a more physical criterion to select the threshold temperature (Eq. (2)), for a general applicability. It is topic of ongoing study.

5.5. After impact X-ray μ -CT observations

A portion of $80 \times 20 \text{ mm}^2$, centred on the impacted area, was taken from some specimens (namely: TP-29k-0.3, TP-48k-0.1, TP-

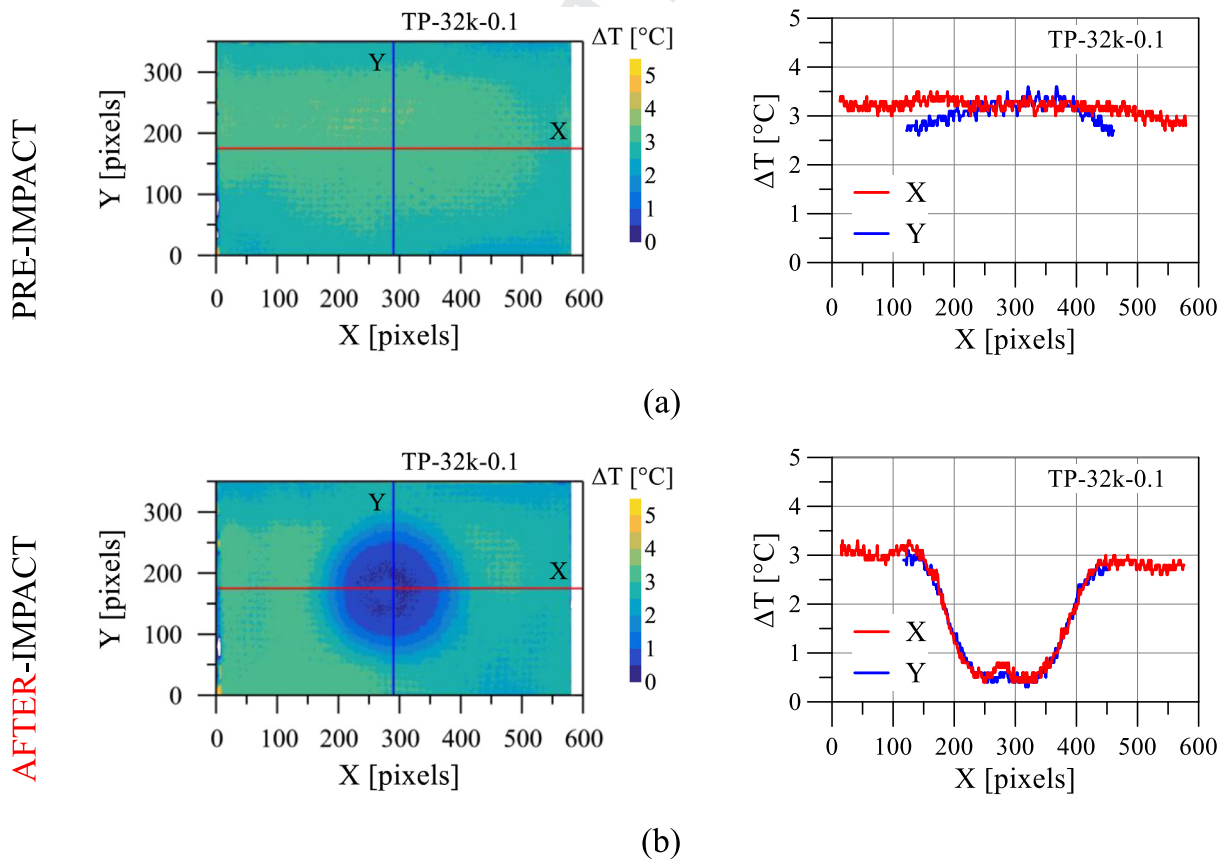


Fig. 14. Representative pre (a) and after (b) impact thermograms (TP-32k-0.1): (left) ΔT distribution on the impacted surface; (right) ΔT along lines X and Y.

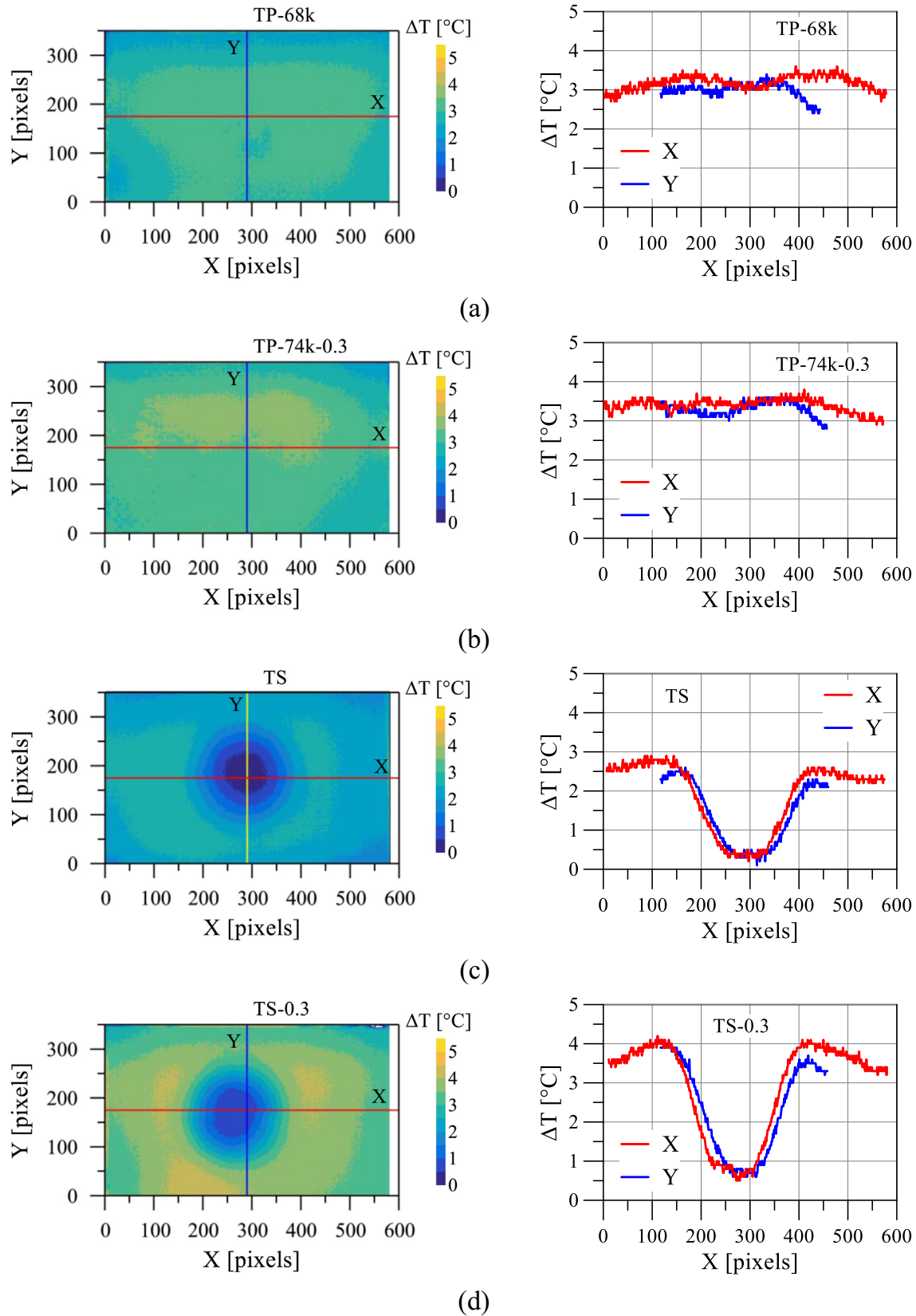


Fig. 15. After impact thermograms: higher Mw (a) unmodified and (b) 0.3% modified TP composites; (c) unmodified and (d) 0.3% modified TS composites. (left) ΔT distribution on the impacted surface; (right) ΔT along lines X and Y.

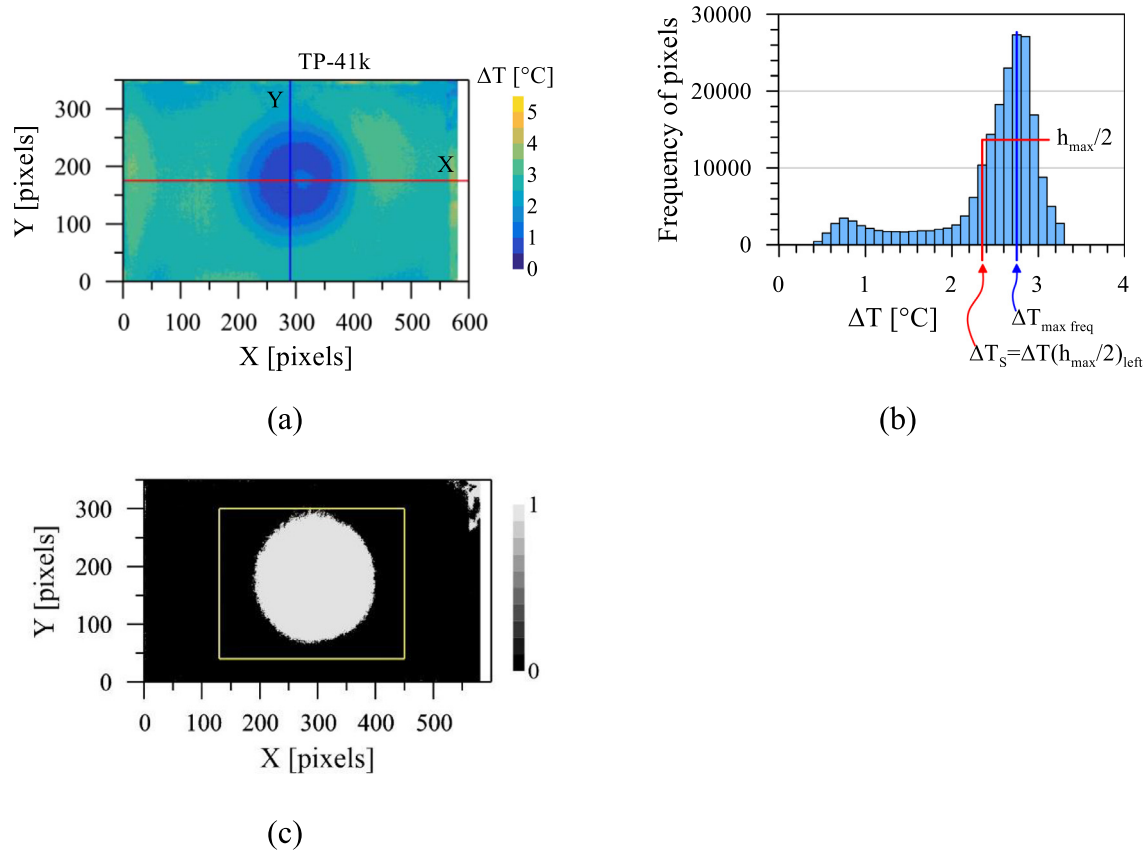


Fig. 16. Preliminary estimation of the damaged area. Steps of the procedure: (a) selected thermogram; (b) histogram of the frequency of pixels' ΔT and setting of the threshold ΔT_S ; (c) map of the damaged area matrix M_D (yellow highlighted box is subdomain for damage area evaluation).

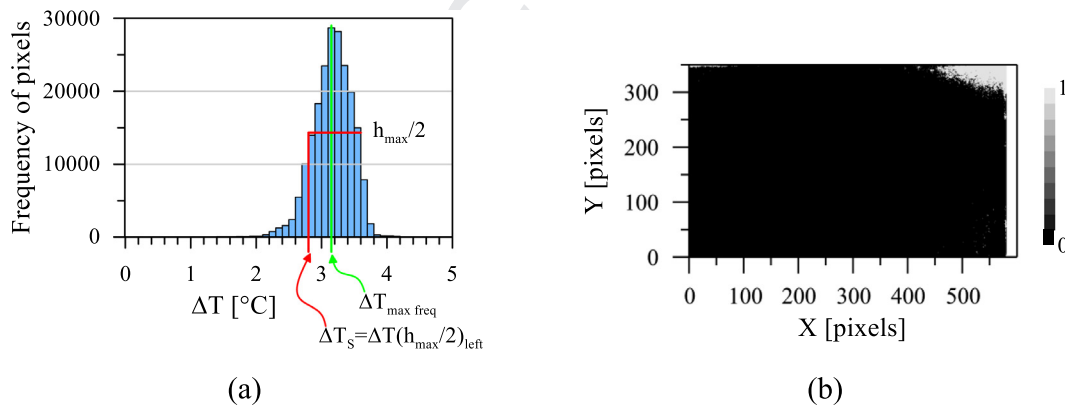


Fig. 17. Preliminary estimation of the damaged area for specimen TP-74k-0.3 (Fig. 15b). (a) Histogram of the frequency of pixels' ΔT and setting of the threshold ΔT_S ; (b) map of the damaged area matrix M_D . No damage detected.

48k-0.3, and TS, TS-0.3), by a diamond saw blade, and then placed in the X-ray μ -CT device. A volume, including the impacted area of size 20 mm \times 20 mm \times thickness, was scanned (see Fig. 19), getting images of size 1000 \times 1000 pixels and resolution of 26.8 μ m/pixel.

The above mentioned mechanical and thermal observations had a counterpart in the damage imparted as observed by the X-ray μ -CT. Typical impact damage mechanisms were observed in the considered composites (Figs. 20–24), namely [3,4]: matrix cracking, fibre-matrix debonding and interlaminar delamination, transverse

bending cracks by tensile flexural stresses, fibre failure under tension and fibre buckling failure under compression. The TS (Fig. 20) composite highlighted a wide distribution of delamination and of transverse cracks passing through the thickness from top to bottom. It had also extensive fibre failure in the tensile region, covering more than half thickness, and compressive fibre failure in the remaining portion of the thickness. The 0.3% content of micro glass fibres in TS composite (Fig. 21) allowed a reduction of delamination, transverse cracks and fibre failure in the compressive region, while similar to TS damage distribution in the tensile portion. As

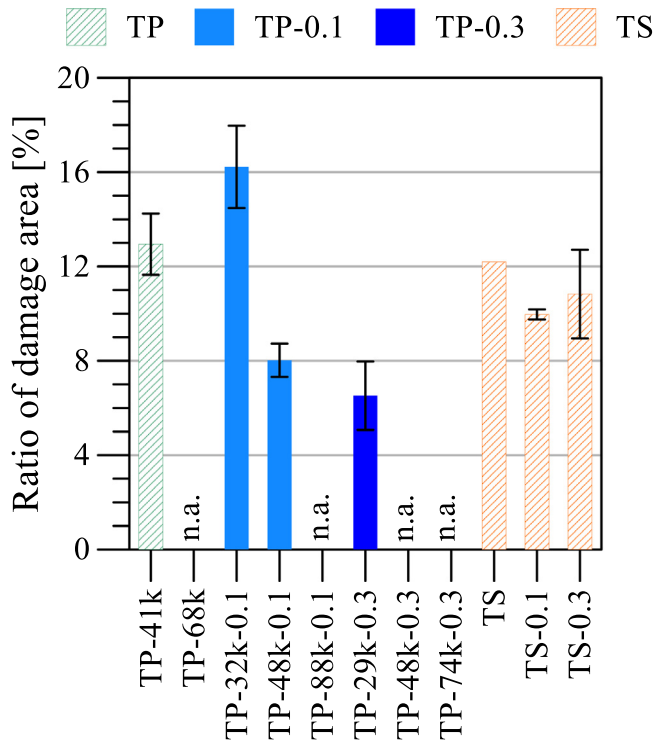


Fig. 18. Preliminary estimation of the damaged area: ratio of damaged area (A_D/A_{Tot}). Average and standard deviation (error bar) of three specimens (two for TS).

for the TS composite, the impact of TS-0.3 generated transverse cracks covering the complete thickness (Fig. 21). The damage pattern observed in the TP of low Mw was very similar to the TS counterpart. In particular, as for the impact properties, the TP-29k with 0.3% of micro glass fibres (Fig. 22) had similar to TS-0.3 distribution of delamination and of fibre failure by tensile and compressive stresses, leading to transverse cracks covering the complete thickness. It shows that the impact damage distribution of the low Mw TP composite, with a reduced fracture toughness, can be improved for some extents by the micro glass fibres, as for the TS composite.

The effect of increasing the Mw with the minimum considered content of micro glass fibre is visible on the damage pattern of composite TP-48k-0.1 (Fig. 23). The coupling of higher Mw and micro fibres reduced the extension of interlaminar delamination and the fibres failure in the compressive zone, comparing to TS and low Mw TP. Although, the failure of fibres in the centre of the impacted area visible over the complete thickness.

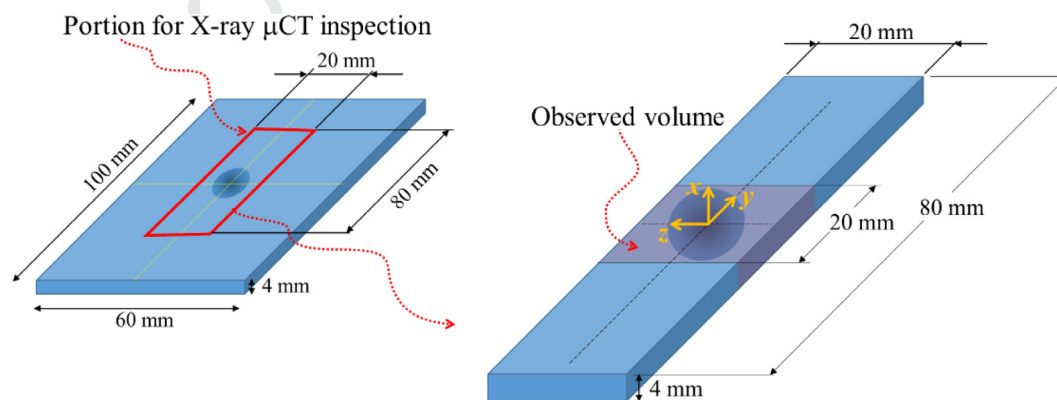


Fig. 19. Portion of the specimen, centred on the impact area, for X-ray μ -CT observations.

Increasing the content of micro glass fibres (0.3%) improves the 'ductile' behaviour of the high Mw TP composite, as detailed above. The composite with 48k Mw TP (Fig. 24) had fewer transverse cracks and interlaminar delamination, as consequence of the better deformability and stress distribution of the matrix. This effect was enhanced by the content of micro fibres, which delayed the cracks propagation, leading to an improve damage tolerance at the laminae level and as consequence to fewer broken fibres and shorter transverse crack paths through the thickness (Fig. 24). The latter justifies the different thermal response of the high Mw TP composite, observed in Section 5.3, with an almost uniform through the thickness heat transfer leading to a more uniform distribution of temperature in the material, which did not allow to thermally distinguish the damage and undamaged portion of the impacted surface.

6. Residual compression strength

The effect of the impact on the mechanical properties of the composites was estimated by comparing the compression strength before and after impact. For some composites, a reduced number of specimens did not allow the compression before impact (see 'n.a.' in Fig. 25). Nevertheless, the obtained results are still of interest and show clear understanding and trend with the available measurements.

The compression strength of TP composites generally increases with the Mw, both before and after impact (Fig. 25).

On the contrary, comparing to the unmodified TS composite, the reduction of strength was of about 50%, insensitive to the modification with micro glass fibres. It is linked to the wide distribution of delamination and of transverse cracks, which was similar with the 0.3% content of micro glass fibres, as highlighted by X-ray μ -CT in the tensile portion (Fig. 21).

Comparing the TP composites with similar medium Mw (41k and 48k), the reduction of strength was 28% for the unmodified matrix, 37% for the 0.1% and 8% for the 0.3% content of micro glass fibres, respectively. The comparison highlights the considerable contribution of the micro glass fibres, mainly with the contents of 0.3%, for the Mw below the transition level (50k–60k, [12]), which reduce the extension of the damage area (see e.g. TP-48k-0.1 in Fig. 18, and Fig. 23) and enhance the after impact compression strength.

For the TP composites of higher Mw, the reduction of strength was 7% for the unmodified matrix (68k), 29% for the 0.1% (88k) and 9% for matrix (74k) with 0.3% content of micro glass fibres. It still indicated the better performance of the TP epoxy composites when coupling higher Mw and micro glass fibres. It reduced the extension of interlaminar delamination and the fibres failure, as

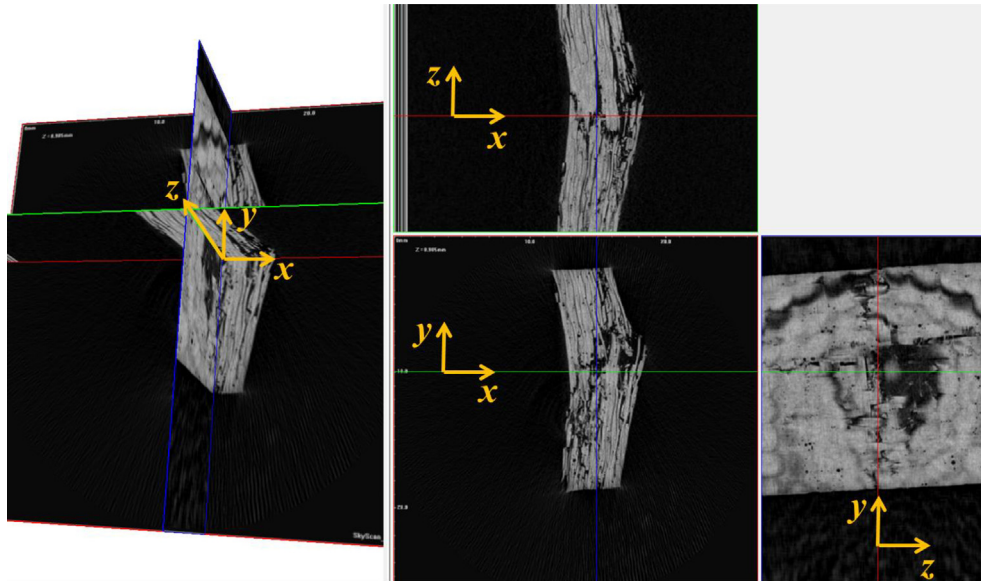


Fig. 20. X-ray μ -CT of a specimen TS.

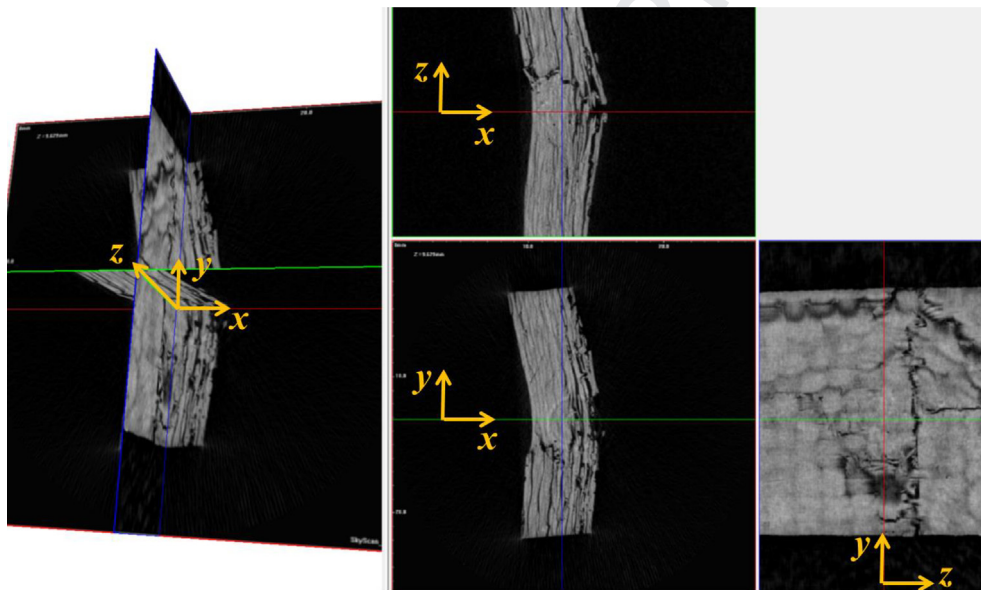


Fig. 21. X-ray μ -CT of a specimen TS-0.3.

observed by X-ray μ -CT (Fig. 24), leading to the higher retention of compression strength.

As for the lower Mw, the low fracture toughness of the composites (Fig. 1) was not enhanced with 0.1% of micro glass fibres (see TP-32k-0.1), leading to the widest damaged area (Fig. 18) and the lowest after impact compression strength (Fig. 25). While increasing the glass fibres content up to 0.3% showed an improved impact damage tolerance of the lower Mw TP composite (see TP-29k-0.3), which had a smaller damaged area and a decrease of the compression strength after impact of 37% comparing to the before impact counterpart.

A general overview of the compression strength after impact highlights: the best after impact performance of the TP epoxy composites, mainly with the medium and high Mw, compared to the TS counterpart; the effectiveness of the micro glass fibres of content 0.3% in improving the retention of mechanical properties of the

low Mw TP composites; the ineffectiveness of the micro glass fibre in the TS epoxy matrix.

7. Conclusions

The experimental study addressed the understanding on the effect of the highly polymerized thermoplastic epoxy matrix and of its hybridization with submicron diameter glass fibres on the impact performance of carbon fibre textile reinforced composite. A thermoset epoxy system was also considered for the sake of comparison. The main outcomes of the investigation can be summarized according to the measurement during impact, the after-impact damage observations and the retention of compressive strength.

Overall, the better impact performance was demonstrated for the high Mw TP composites, unmodified and 0.3% modified matri-

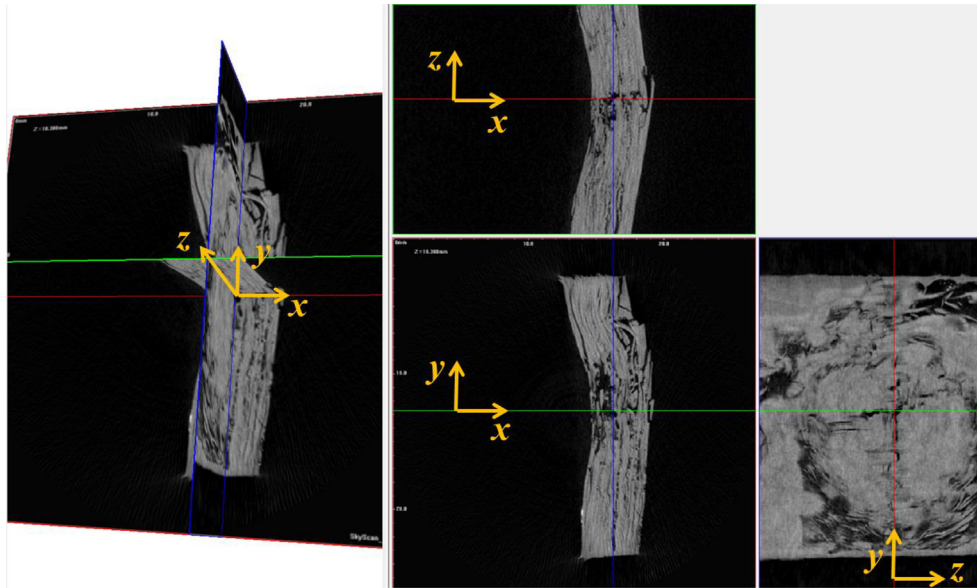


Fig. 22. X-ray μ -CT of a specimen TP-29k-0.3.

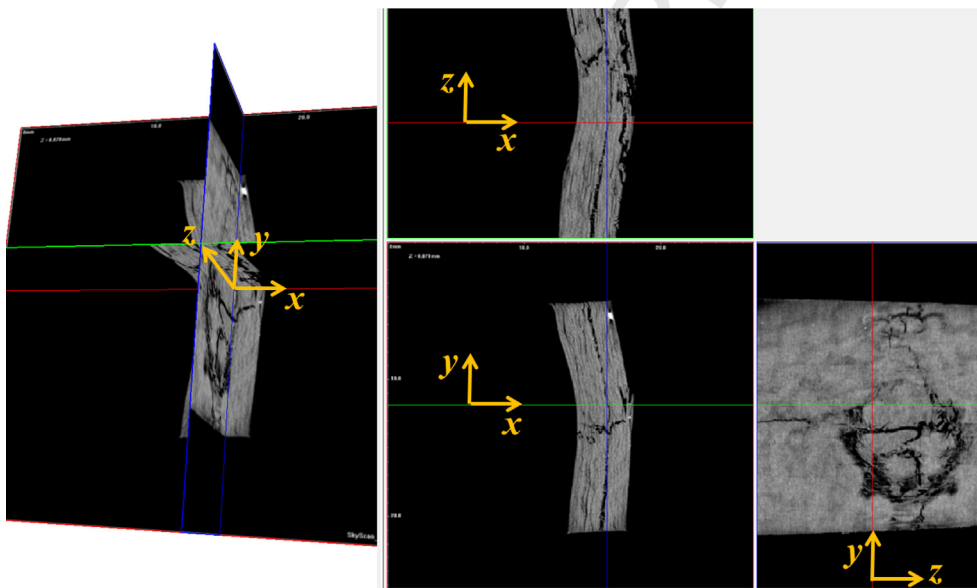


Fig. 23. X-ray μ -CT of a specimen TP-48k-0.1.

733 ces, which had smooth and more 'ductile' post peak impact force
 734 behaviour and the lower level of absorbed energy than the TS
 735 counterparts. It was connected to the relative lower energy dedi-
 736 cated to the damage propagation. The damage distribution was
 737 observed on the impacted surface by the laser morphology and
 738 the infrared thermography, as well as inside the material by the
 739 X-ray μ -CT. All observations and measurements confirmed the bet-
 740 ter damage performance of the high Mw TP composites, mainly
 741 when combined with 0.3% of micro glass fibres. They had reduced
 742 residual deformation (dent depth), and an almost uniform distribu-
 743 tion of the surface temperature, completely different than the one
 744 of TS and low Mw TP composites. Those external measurements
 745 had a strong support and explanations observing the damage
 746 inside the composites. The micro glass fibres (0.3%) in the high

Mw TP was responsible of the lower crack density and interlaminar
 delamination, leading to an improved damage tolerance with a
 reduced number of broken fibres and shorter transverse crack
 paths thought the thickness.

As for the retention of compressive strength, the TP epoxy com-
 posites had the best after impact performance, mainly with the
 medium and high Mw, compared to the TS counterpart. The micro
 glass fibres of content 0.3% were ineffective in the TS epoxy matrix,
 while considerably enhanced the after-impact reduction of com-
 pressive strength of the low Mw TP composites.

Finally, the investigation pointed out the ability of the high Mw
 thermoplastic epoxy matrix and of the proper content (0.3%) of
 submicron diameter glass fibres to enhance the impact resistance
 of the carbon reinforced composites, which, coupled with the

747
748
749
750
751
752
753
754
755
756
757
758
759
760

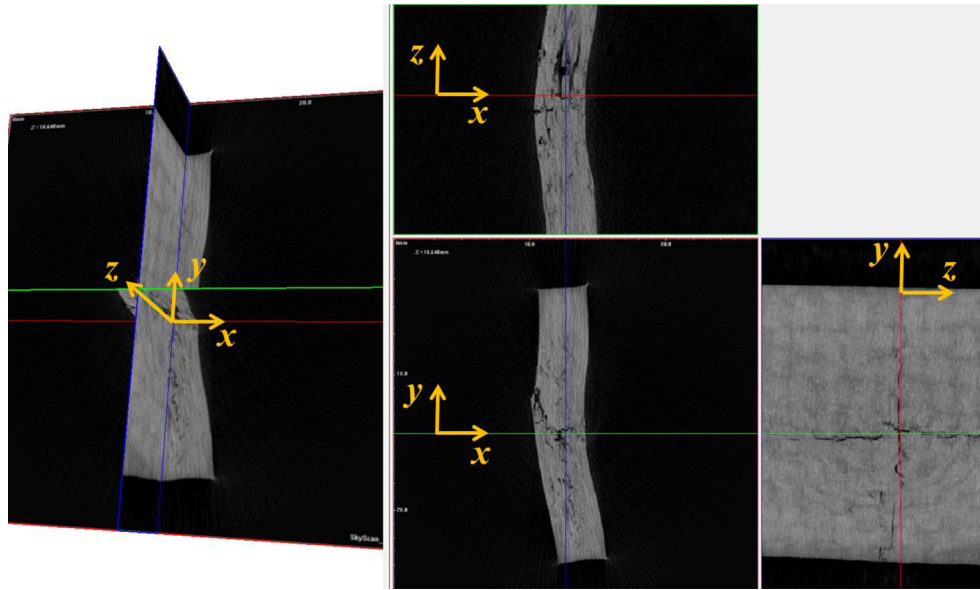


Fig. 24. X-ray μ -CT of a specimen TP-48k-0.3.

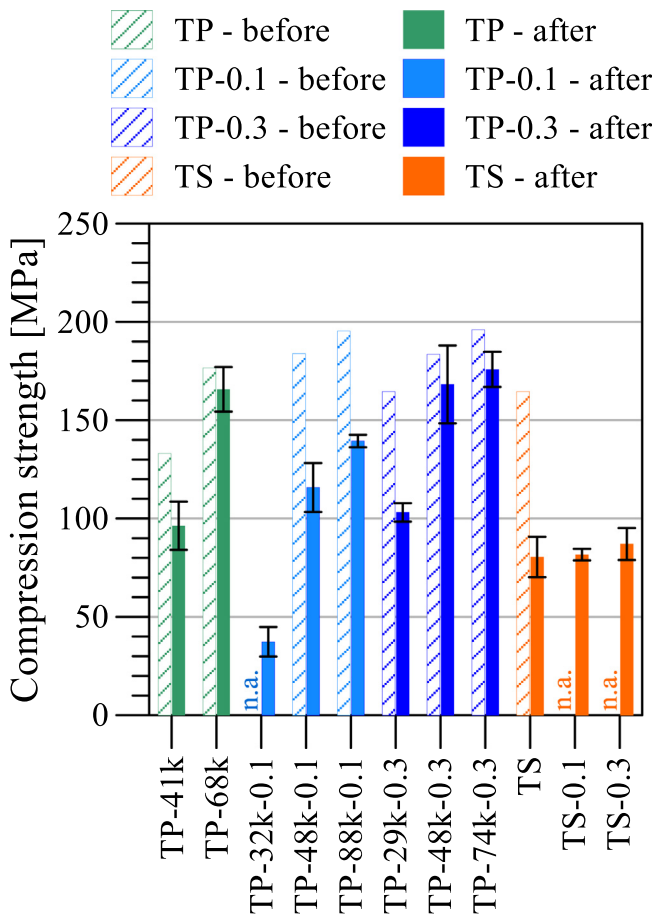


Fig. 25. Compression strength, before and after impact, average and standard deviation (error bar) of two (before impact) and three (after impact) specimens.

improvement of other mechanical properties ([12]), highlighted the applicability of the highly polymerized thermoplastic epoxy for composite materials in several industrial applications.

CRediT authorship contribution statement

Valter Carvelli: Conceptualization, Data curation, Formal analysis, Investigation, Methodology, Validation, Writing - original draft, Writing - review & editing. **Hironori Nishida:** Investigation, Methodology, Validation, Writing - review & editing. **Toru Fujii:** Methodology, Supervision, Funding acquisition, Project administration, Writing - review & editing. **Kazuya Okubo:** Methodology, Supervision, Writing - review & editing.

Declaration of Competing Interest

The authors declare that they have no known competing financial interests or personal relationships that could have appeared to influence the work reported in this paper.

Acknowledgement

The authors are grateful for support of Doshisha University Research & Development Center for Advanced Composite Materials and Nagase Chemtex Corporation, Japan. Souichirou Imagawa and Taiki Ueda are gratefully acknowledged for performing some experimental activities.

Funding

This work was (partially) supported by JSPS Grant-in-Aid for Scientific Research (B), Grant Number JP18H01343.

References

- [1] Safri SNA, Sultan MTH, Jawaid M, Jayakrishna K. Impact behaviour of hybrid composites for structural applications: a review. *Compos B* 2018;133:112-21. <https://doi.org/10.1016/j.compositesb.2017.09.008>.
- [2] Shah SZH, Karuppanan S, Megat-Yusoff PSM, Sajid Z. Impact resistance and damage tolerance of fiber reinforced composites: a review. *Compos Struct* 2019;217:100-21. <https://doi.org/10.1016/j.compstruct.2019.03.021>.
- [3] Jefferson Andrew J, Srinivasan SM, Arockiarajan A, Dhakal Hom Nath. Parameters influencing the impact response of fiber-reinforced polymer matrix composite materials: a critical review". *Compos Struct* 2019;224: <https://doi.org/10.1016/j.compstruct.2019.111007>.
- [4] Agrawal S, Kumar Sing K, Sarkar PK. Impact damage on fibre-reinforced polymer matrix composite - a review. *J Compos Mater* 2014;48:317-32. <https://doi.org/10.1177/0021998312472217>.

- [5] Grogan J, Tekalur SA, Shukla A, Bogdanovich A, Coffelt RA. Ballistic resistance of 2D and 3D woven sandwich composites. *J Sandwich Struct Mater* 2007;9:283–302. <https://doi.org/10.1177/1099636207067133>.
- [6] Aymerich F, Priolo P. Characterization of fracture modes in stitched and unstitched cross-ply laminates subjected to low-velocity impact and compression after impact loading. *Int J Impact Eng* 2008;35:591–608. <https://doi.org/10.1016/j.ijimpeng.2007.02.009>.
- [7] Hart KR, Chia PXL, Sheridan LE, Wetzel ED, Sottos NR, White SR. Mechanisms and characterization of impact damage in 2D and 3D woven fiber-reinforced composites. *Compos A* 2017;101:432–43. <https://doi.org/10.1016/j.compositesa.2017.07.004>.
- [8] Cartié DDR, Irving PE. Effect of resin and fibre properties on impact and compression after impact performance of CFRP. *Compos A* 2002;33:483–93. [https://doi.org/10.1016/S1359-835X\(01\)00141-5](https://doi.org/10.1016/S1359-835X(01)00141-5).
- [9] Domun N, Kaboglu C, Paton KR, Dear JP, Liu J, Blackman BRK, et al. Ballistic impact behaviour of glass fibre reinforced polymer composite with 1D/2D nanomodified epoxy matrices. *Compos B* 2019;167:497–506. <https://doi.org/10.1016/j.compositesb.2019.03.024>.
- [10] Yudhanto A, Wafai H, Lubineau G, Goutham S, Mulle M, Yaldiz R, et al. Revealing the effects of matrix behavior on low-velocity impact response of continuous fiber-reinforced thermoplastic laminates. *Compos Struct* 2019;210:239–49. <https://doi.org/10.1016/j.compstruct.2018.11.040>.
- [11] Nagase ChemteX Corporation. Process for Production of Thermoplastic Cured Epoxy Resin with Transparency to Visible Light, and Thermoplastic Epoxy Resin Composition. United States Patent US 2014/0194590 A1; 2014.
- [12] Nishida H, Carvelli V, Fujii T, Okubo K. Quasi-static and fatigue performance of carbon fibre reinforced highly polymerized thermoplastic epoxy. *Compos B* 2018;144:163–70. <https://doi.org/10.1016/j.compositesb.2018.03.002>.
- [13] Kostopoulos V, Tsotra P, Karapappas P, Tsantalis S, Vavouliotis A, Loutas TH, et al. Mode I interlaminar fracture of CNF or/and PZT doped CFRPs via acoustic emission monitoring. *Compos Sci Technol* 2007;67:822–8. <https://doi.org/10.1016/j.compscitech.2006.02.038>.
- [14] Tang Y, Ye L, Zhang Z, Friedrich K. Interlaminar fracture toughness and CAI strength of fibre-reinforced composites with nanoparticles – a review. *Compos Sci Technol* 2013;86:26–37. <https://doi.org/10.1016/j.compscitech.2013.06.021>.
- [15] Quaresimin M, Varley RJ. Understanding the effect of nano-modifier addition upon the properties of fibre reinforced laminates. *Compos Sci Technol* 2008;68:718–26. <https://doi.org/10.1016/j.compscitech.2007.09.005>.
- [16] De Greef N, Gorbatiikh L, Godara A, Mezzo L, Lomov SV, Verpoest I. The effect of carbon nanotubes on the damage development in carbon fiber/epoxy composites. *Carbon* 2011;49:4650–64. <https://doi.org/10.1016/j.carbon.2011.06.047>.
- [17] Sprenger S. Fiber-reinforced composites based on epoxy resins modified with elastomers and surface-modified silica nanoparticles. *J Mater Sci* 2014;49:2391–402. <https://doi.org/10.1007/s10853-013-7963-8>.
- [18] Carvelli V, Betti A, Fujii T. Fatigue and Izod impact performance of carbon plain weave textile reinforced epoxy modified with cellulose microfibrils and rubber nanoparticles. *Compos A* 2016;84:26–35. <https://doi.org/10.1016/j.compositesa.2016.01.005>.
- [19] Nash NH, Young TM, McGrail PT, Stanley WF. Inclusion of a thermoplastic phase to improve impact and post-impact performances of carbon fibre reinforced thermosetting composites—a review. *Mater Des* 2015;85:582–97. <https://doi.org/10.1016/j.matdes.2015.07.001>.
- [20] Zhao Q, Hoa SV. Toughening mechanism of epoxy resins with micro/nano particles. *J Compos Mater* 2007;41:201–19. <https://doi.org/10.1177/0021998306063361>.
- [21] Bunea M, Cîrciumaru A, Buciumeanu M, Bîrsan IG, Silva FS. Low velocity impact response of fabric reinforced hybrid composites with stratified filled epoxy matrix. *Compos Sci Technol* 2019;169:242–8. <https://doi.org/10.1016/j.compscitech.2018.11.024>.
- [22] Hudnut SW, Chung DDL. Use of submicron diameter carbon filaments for reinforcement between continuous carbon fiber layers in a polymer-matrix composite. *Carbon* 1995;33:1627–31. [https://doi.org/10.1016/0008-6223\(95\)00148-7](https://doi.org/10.1016/0008-6223(95)00148-7).
- [23] Nishida H. The development of thermoplastic epoxy resin and continuous fiber reinforced thermoplastics using it. *J Adhesion Soc Japan* 2015;51:516–23. <https://doi.org/10.11618/adhesion.51.516>.
- [24] H. Nishida, V. Carvelli, T. Fujii, K. Okubo, Thermoplastic vs. thermoset epoxy carbon textile composites. In: 13th International Conference on Textile Composites (TEXCOMP-13), Milan, 17–19 September 2018, IOP Conference Series: Materials Science and Engineering, vol. 406, 2018. <https://doi.org/10.1088/1757-899X/406/1/0120439>.
- [25] JIS K 7086, Testing methods for interlaminar fracture toughness of carbon fibre reinforced plastics, Japanese Standards Association, 2018.
- [26] ISO 180. Plastics – Determination of Izod impact strength, International Organization for Standardization, 2000.
- [27] ASTM D7136M-15. Standard test method for measuring the damage resistance of a fiber-reinforced polymer matrix composite to a drop-weight impact event, West Conshohocken, PA: ASTM International, 2015.
- [28] ASTM D7137M-17. Standard test method for compressive residual strength properties of damaged polymer matrix composite plates, West Conshohocken, PA: ASTM International, 2017.
- [29] Li Y, Zhang W, Ming A-B, Yang Z-W, Tian G. A new way for revealing the damage evolution of impacted CFRP laminate under compression-compression fatigue load based on thermographic images. *Compos Struct* 2017;176:1–8. <https://doi.org/10.1016/j.compstruct.2017.05.009>.
- [30] Maierhofer C, Krankenhagen R, Röllig M. Application of thermographic testing for the characterization of impact damage during and after impact load. *Compos B* 2019;173:.. <https://doi.org/10.1016/j.compositesb.2019.106899>106899.

845
846
847
848
849
850
851
852
853
854
855
856
857
858
859
860
861
862
863
864
865
866
867
868
869
870
871
872
873
874
875
876
877
878
879
880
881
882
883
884
885
886
887
888
889
890